nemo-like kinase is an essential co-activator of Wnt signaling during early zebrafish development

Chris J. Thorpe and Randall T. Moon*

Howard Hughes Medical Institute, Department of Pharmacology and Center for Developmental Biology, Box 357750, University of Washington School of Medicine, Seattle, WA 98195, USA
*Author for correspondence (e-mail: rtmoon@u.washington.edu)

Accepted 15 March 2004

Development 131, 2899-2909
Published by The Company of Biologists 2004
doi:10.1242/dev.01171

Summary

Wnt/β-catenin signaling regulates many aspects of early vertebrate development, including patterning of the mesoderm and neurectoderm during gastrulation. In zebrafish, Wnt signaling overcomes basal repression in the prospective caudal neurectoderm by Tcf homologs that act as inhibitors of Wnt target genes. The vertebrate homolog of *Drosophila nemo*, nemo-like kinase (*Nlk*), can phosphorylate Tcf/Lef proteins and inhibit the DNA-binding ability of β-catenin/Tcf complexes, thereby blocking activation of Wnt targets. By contrast, mutations in a *C. elegans* homolog show that Nlk is required to activate Wnt targets that are constitutively repressed by Tcf. We show that overexpressed zebrafish *nlk*, in concert with *wnt8*, can downregulate two *tcf3* homologs, *tcf3a* and *tcf3b*, that repress Wnt targets during neurectodermal patterning. Inhibition of *nlk* using morpholino oligos reveals essential roles in regulating ventrolateral mesoderm formation in conjunction with *wnt8*, and in patterning of the midbrain, possibly functioning with *wnt8b*. In both instances, *nlk* appears to function as a positive regulator of Wnt signaling. Additionally, *nlk* strongly enhances convergent/extension phenotypes associated with *wnt11*/*silberblick*, suggesting a role in modulating cell movements as well as cell fate.

Key words: Nemo-like kinase, Wnt, Zebrafish, Tcf, Lef

Introduction

Wnt proteins comprise a family of secreted signaling molecules that perform essential roles in numerous processes during animal development. In early vertebrate embryos, Wnt signaling pathways have been implicated in axis specification, cell proliferation, mesoderm and neuroectoderm patterning, and in the regulation of cell movement during gastrulation (reviewed by Cadigan and Nusse, 1997; Peifer and Polakis, 2000; Veeman et al., 2003). Intensive study of the different roles of Wnt signals and their underlying molecular mechanisms has led to a general grouping of Wnt pathways into two classes: canonical (β-catenin dependent) and non-canonical (β-catenin independent) (reviewed by Veeman et al., 2003). Canonical Wnt signaling functions via the stabilization of cytoplasmic pools of β-catenin, which is constitutively degraded in the absence of Wnt signaling. Stabilized β-catenin then translocates to the nucleus and interacts with members of the Tcf/Lef family of transcription factors. Tcf/Lef proteins bound alone to DNA can repress transcription because of their binding of general repressors such as Groucho and CtBP. β-catenin contains transcriptional transactivation domains, so it is thought that by binding to Tcf/Lef proteins bound to DNA, β-catenin converts the repressive Tcf/Lef to an activator.

Recently, evidence that canonical Wnt signaling can be regulated by MAP kinase signaling has emerged. Genetic analysis of endoderm specification in the early *C. elegans* embryo demonstrates an essential requirement for both Wnt signaling and a MAPK-related pathway for proper specification of endodermal fate (Meneghini et al., 1999; Rocheleau et al., 1997; Rocheleau et al., 1999; Thorpe et al., 1997). Two of the genes involved in this process, *lit-1* and *mom-4*, encode homologs of the *Drosophila* MAPK-related gene *nemo* and vertebrate TGFβ-activated kinase (Tak1), respectively. Epistasis studies have shown that a *C. elegans* Tcf/Lef homolog, *pop-1*, represses endoderm fates, and that this repression is relieved by the combinatorial action of Wnt signaling and a parallel pathway involving *lit-1/nemo* and *mom-4/Tak1*, permitting endoderm development (Meneghini et al., 1999; Rocheleau et al., 1997; Rocheleau et al., 1999; Shin et al., 1999; Thorpe et al., 1997). Studies of a mouse homolog of *lit-1*/*nemo*, nemo-like kinase (*Nlk*), in mammalian cell culture also demonstrate that Nlk and Tak1 can regulate activation of Wnt targets (Ishitani et al., 2003b; Ishitani et al., 1999). Biochemical studies indicate that Tak1 activates Nlk, which can then phosphorylate Tcf, inhibiting the DNA-binding ability of β-catenin/Tcf complexes (Ishitani et al., 2003b; Ishitani et al., 1999; Rocheleau et al., 1999).

In different contexts, Nlk proteins can function as either inhibitors or activators of Wnt target genes. For example, in the early *C. elegans* embryo, the eventual outcome of the Wnt signal may be to simply derepress genes that are inhibited by Tcf proteins (for reviews, see Behrens, 2000; Thorpe et al., 2000). Following the elimination of the repressive activity of *pop-1*/Tcf by *lit-1*/Nlk and *wrm-1*/β-catenin, other elements within the promoter can drive transcription. For example, two GATA factors, *med-1* and *med-2*, can initiate transcription of the earliest endoderm-specific genes when *pop-1* repression is relieved (Maduro et al., 2001).

In other contexts, where a β-catenin/Tcf complex is required to directly activate transcription, phosphorylation of Tcf by Nlk and subsequent inhibition of DNA binding of the β-catenin/Tcf complex would block activation, as is shown in experiments where Nlk blocks activation of the Wnt-responsive TOPFLASH reporter (Ishitani et al., 2003b; Ishitani et al., 1999). Also, injection of mouse or *Xenopus Nlk* RNA into *Xenopus* embryos blocks duplication of the dorsal axis induced by Wnt or β-catenin (Hyodo-Miura et al., 2002; Ishitani et al., 1999).

A role for Wnt signaling in overcoming Tcf-mediated repression has recently been described in zebrafish (Kim et al., 2000; Dorsky et al., 2003). A Tcf3 homolog, encoded by the *headless (hdl)* gene, is required to repress Wnt signaling during neural patterning (Kim et al., 2000). *wnt8* is required during gastrulation to induce posterior neural fates (Erter et al., 2001; Fekany-Lee et al., 2000; Lekven et al., 2001), and this posteriorizing activity is opposed in prospective anterior neuroectoderm by *hdl*/*tcf3a* (Kim et al., 2000). *hdl*/*tcf3a* mutant embryos lack anterior neural structures and have expanded posterior neural fates, consistent with ectopic Wnt signaling. Inhibition of *tcf3a* results in expanded posterior neural fates even in the absence of *wnt8* function, supporting a model in which Wnt signaling functions solely to derepress Tcf-inhibited genes (Dorsky et al., 2003). Furthermore, a truncated Tcf3a protein that cannot bind β-catenin and can thus only act as a repressor completely rescues the *hdl* mutant (Kim et al., 2000). To determine whether the cooperative function of Nlk and Wnt signaling in derepressing Tcf-inhibited genes was conserved from nematodes to teleost fish, we undertook an analysis of Nlk function in zebrafish embryos.

Materials and methods

Zebrafish maintenance and in situ hybridization

Zebrafish were raised and maintained under standard conditions. In situ hybridization using digoxigenin-labeled mRNA probes was performed using standard methods (Oxtoby and Jowett, 1993).

Cloning of *nlk*

We used degenerate PCR on a 24-hour-stage cDNA library, followed by 5′ and 3′ RACE using the SMART RACE kit (Clontech), to amplify a cDNA containing the entire *nlk* ORF, plus 170 base pairs (bp) of 5′ UTR and 574 bp of 3′UTR sequence. This sequence was deposited in GenBank (Accession Number AY562552). For in situ hybridization, a fragment containing the complete ORF, plus 62 bp of 5′ UTR and 130 bp of 3′ UTR was amplified and ligated into pGEM-T (Promega). For mRNA synthesis, we designed primers corresponding to the 5′ and 3′ ends of the ORF, and inserted the full-length product into pCS2+ (Turner and Weintraub, 1994). The *nlk* point mutants, *nlk* (K117M) and *nlk* (C387Y), were constructed using standard PCR-based site-directed mutagenesis.

mRNA and morpholino injections

For mRNA injections, sense transcripts were synthesized using the mMessage mMachine kit (Ambion). For templates, we used full-length cDNA inserted into pCS2+. mRNA was resuspended in water or Danieau's buffer prior to injection. Morpholino antisense oligonucleotides (*nlk*: 5′-GTGTGTGGTACCTTAAGCAGACAGT-3′) were obtained from Gene Tools (Philomath, OR). *tcf3b*, *lef1*, *wnt8b*, *wnt11*, wnt8 ORF1 and *wnt8* ORF2 morpholinos have been previously described (Dorsky et al., 2003; Dorsky et al., 2002; Houart et al., 2002; Lekven et al., 2001; Lele et al., 2001). The standard control morpholino provided by Gene Tools was used in some experiments. Morpholinos were dissolved in Danieau's buffer (Nasevicius and Ekker, 2000) prior to use. For all injections, 2-3 nl of a 1 ng/nl stock was injected at the one-cell stage, except where otherwise noted.

Results

Cloning of zebrafish *nlk*

We used degenerate PCR on a 24-hour-stage zebrafish cDNA library, then 5′ and 3′ RACE to amplify a full-length open reading frame for *nlk*. The predicted protein sequence is most similar to a recently identified *Xenopus* Nlk (76% identical, 83% similar). A protein sequence alignment between zebrafish, frog and human Nlks shows that all three proteins are highly homologous throughout the predicted kinase domains, but are very divergent over the first 100 residues (Fig. 1A).

Expression of *nlk* during embryogenesis

RT-PCR analysis (data not shown) shows that *nlk* is expressed maternally and throughout the first day of development. By in situ hybridization, *nlk* is expressed strongly and ubiquitously throughout gastrulation stages (Fig. 1B and data not shown). At tailbud stage, *nlk* is still expressed throughout the embryo, but the presumptive notochord shows higher levels of expression (Fig. 1C, arrowhead). During somitogenesis (Fig. 1D,E), *nlk* expression is observed exclusively in the neural tube, including in the eyes by 24 hours post-fertilization (hpf). Expression of *nlk* is more restricted at 48 hpf, becoming localized to the otic vesicles (Fig. 1F, arrowheads) and the ganglion cell layer of the retina (arrow), as well as to unidentified regions of the ventral brain.

nlk RNA overexpression results in loss of anterior neural fates

As a first test to assess the activity of *nlk* during early development, we injected in vitro-transcribed *nlk* mRNA into one-cell zebrafish embryos. Injection of 200 pg *nlk* RNA results in embryos with variable loss of eyes and forebrain (Fig. 2D and data not shown), and no other obvious morphological abnormalities at 24 hpf (59% of embryos have small or missing eyes; *n*=510). Changing a conserved cysteine residue to tyrosine at amino acid 425 in mouse Nlk eliminates its ability to bind Tcf (Ishitani et al., 1999). We made the analogous change in zebrafish *nlk* (C387Y) and found that injection of this mutated RNA had almost no effect on development (1% of embryos had small eyes; *n*=190), suggesting that the *nlk* overexpression phenotype is dependent on interaction with Tcf proteins. Furthermore, we constructed *nlk* (K117M), analogous to mouse *Nlk* (K155M), which is kinase dead and unable to block Tcf binding to DNA (Ishitani et al., 1999). Injection of *nlk* (K117M) RNA has no effect on development (2% of embryos had small eyes; *n*=109), indicating that the kinase activity of *nlk* is required to induce the loss of anterior neural structures.

nlk RNA enhances *tcf3a* and *tcf3b* loss-of-function phenotypes

Two zebrafish Tcf3-related genes, *tcf3a* and *tcf3b*, have been shown to cooperatively regulate AP patterning in the neurectoderm by repressing posterior neural fates (Dorsky et

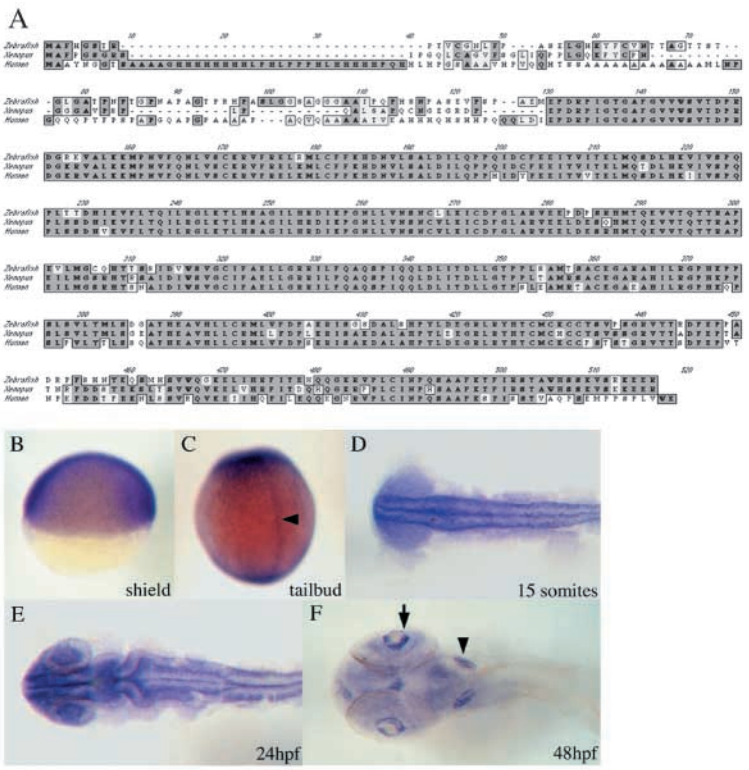

Fig. 1. *nlk* encodes a protein that is highly homologous to other vertebrate Nlks, and is expressed broadly throughout development. (A) CLUSTAL alignment of zebrafish, *Xenopus* and human Nlk proteins. Identical amino acids are shaded in dark gray; similar residues are in light gray. All three proteins are extremely highly conserved throughout most of the sequence, but are highly divergent near the N terminus. Overall, zebrafish Nlk is most similar to *Xenopus* Nlk. (B-F) *nlk* in situ hybridization. (B) Lateral view of a shield stage embryo, dorsal to the right, showing ubiquitous *nlk* expression. (C) Dorsal view of a tailbud stage embryo. *nlk* is broadly expressed, but higher levels are seen in the prospective notochord (arrowhead). (D) Dorsal view of a flat-mounted embryo at 15 somites. *nlk* is highly expressed throughout the CNS, excluding the developing eyes. (E) Dorsal view of a flattened embryo at 24 hours shows intense staining in the eyes, in addition to continued strong staining elsewhere in the CNS. (F) Ventral view of a 48 hpf embryo. *nlk* transcripts are localized to the otic vesicles (arrowhead), and in the ganglion cell layer of the retina (arrow).

al., 2003). In *tcf3a* mutants, posterior neural fates expand at the expense of anterior fates, causing embryos to develop lacking telencephalon and eyes (Kim et al., 2000). Although *tcf3b* morphants do not show any defects in AP patterning of the neurectoderm, the *tcf3a* phenotype is enhanced when *tcf3b* is also inhibited, suggesting that the two genes function redundantly (Dorsky et al., 2003). Given the similarity between the *nlk* overexpression and the *tcf3a* loss-of-function phenotypes, as well as the established role for the *C. elegans* Nlk homolog in derepression of *tcf*-inhibited genes, we reasoned that *nlk* was likely to be interacting with one or both of the zebrafish Tcf3 homologs. We therefore compared the effects of *nlk* overexpression and *tcf3* loss of function on neural markers, and also examined the ability of *nlk* overexpression to enhance the phenotypes due to loss of either *tcf3* homolog alone (Fig. 2).

Injection of *tcf3a* MO results in a loss of telencephalon and eyes at 24 hpf (Fig. 2G, compare with wild type in Fig. 2A), and caused an expansion of the midbrain/hindbrain boundary (MHB) domain of *pax2* (Fig. 2H) and a decrease in the diencephalic expression of *pax6* (Fig. 2I), reflecting the increase in caudal character of the neurectoderm. Injection of *tcf3b* MO caused only a disorganization of the hindbrain (Fig. 2J); both *pax2* and *pax6* expression was normal (Fig. 2K,L). Co-injection of both *tcf3* morpholinos strongly enhanced the *tcf3a* phenotype, eliminating the morphological MHB at 24 hpf (Fig. 2M), greatly expanding *pax2* expression, and eliminating *pax6* expression (Fig. 2N,O).

Injection of 200 pg of *nlk* RNA results in anterior truncations like those seen in *tcf3a* morphants (Fig. 2D). Similar to *tcf3a* morphants, *pax2* expression is expanded and *pax6* expression is reduced (Fig. 2E,F). *nlk* overexpression, then, phenocopies inhibition of *tcf3a* function, suggesting that *nlk* can negatively regulate the repression of posterior neural genes by *tcf3a*. Co-injection of 100 pg *tcf3a* RNA resulted in significant rescue of the *nlk* overexpression phenotype [62% (*n*=63) of *nlk*/*tcf3a* RNA-injected embryos had normal *pax2* expression at 3 somites versus 31% (*n*=51) of *nlk*/GFP RNA-injected embryos], further indicating that the *nlk* overexpression phenotype is due to downregulation of *tcf3a*. Although most *nlk*-injected embryos closely resemble *tcf3a* morphants, when we injected high doses (800 pg) of *nlk* RNA, we saw embryos with a slightly more severe phenotype, but not to the degree seen in *tcf3a*/*tcf3b* double morphants (data not shown). This suggests that although *nlk* may preferentially interact with *tcf3a*, it may also be able to inhibit *tcf3b* to some degree. To test this, we co-injected *nlk* RNA with either *tcf3a* or *tcf3b* morpholinos. If *nlk* can downregulate *tcf3b* in addition to *tcf3a*, then co-injection of *nlk* RNA and *tcf3a* MO should phenocopy *tcf3a*/*tcf3b* morphants, showing both the dramatic expansion of *pax2* and the loss of diencephalic *pax6* expression. Indeed, nearly every embryo shows a more severe phenotype than that seen by injection of *nlk* RNA alone, with most phenocopying *tcf3a/tcf3b* morphants (82%; *n*=73; Fig. 2P,Q,R, compare with Fig. 2M,N,O). Most *nlk* RNA/*tcf3b* MO embryos also show the more severe phenotype characteristic of *tcf3a/3b* morphants (89% of embryos completely lack *pax6*; *n*=54; Fig. 2S,T,U). These results indicate that *nlk* is capable of interacting with both *tcf3a* and *tcf3b* to relieve their repression of posterior neural genes.

nlk requires *wnt8* signaling to posteriorize neurectoderm

The *nlk* phenotype is similar to that seen with injection of low levels (5-10 pg) of zebrafish *wnt8* RNA (Kelly et al., 1995). *wnt8* is required to induce posterior fates within the

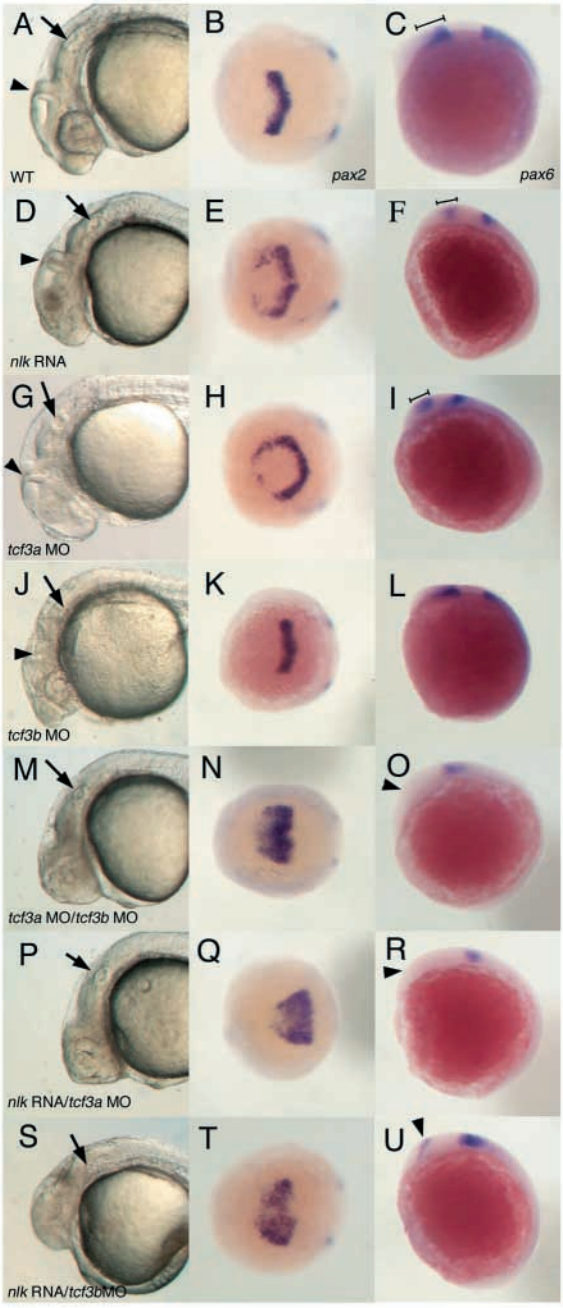

Fig. 2. *nlk* RNA synergizes with *tcf3a* or *tcf3b* MOs. Comparison of wild-type (WT; A,B,C), *nlk* RNA (D,E,F), *tcf3a* MO (G,H,I), *tcf3b* MO (J,K,L), *tcf3a*/*tcf3b* MOs (M,N,O), *nlk* RNA/*tcf3a* MO (P,Q,R) and *nlk* RNA/*tcf3b* MO (S,T,U) embryos. *nlk* RNA (200 pg) was injected in conjunction with 1-2 ng of each of indicated morpholino. Control morpholino (see Materials and methods) was included to balance out the total amount of morpholino injected in each experiment. The first column shows lateral views of the head at 24 hours, with arrows indicating the otic vesicle and arrowheads marking the midbrain/hindbrain boundary (MHB). The middle column shows a dorsal view of embryos fixed at the 2 to 3 somite stage and stained with *pax2* probe, whereas the last column shows lateral views of *pax6* expression at 3 somites. In *nlk* RNA (D) and *tcf3a* MO (G) embryos, the eyes are missing, but embryos still develop a clear MHB, compared with wild type (A). *pax2* expression is expanded in both *nlk* RNA (E) and *tcf3a* MO (H) embryos. *pax6* expression in the diencephalon (marked by brackets in C,F,I) is slightly reduced in *nlk* RNA (F) and *tcf3a* MO (I) embryos relative to wild type (C). tcf3b MO embryos show a disorganization of the hindbrain (J), but still make eyes, and have normal *pax2* and *pax6* expression (K,L). Co-injection of *tcf3a* and *tcf3b* MOs results in more severe anterior truncations, with no visible MHB (M), a greatly expanded *pax2* expression domain (N), and elimination of diencephalic *pax6* (O, arrowhead). Co-injection of *nlk* RNA with either *tcf3a* MO (P,Q,R) or *tcf3b* MO (S,T,U) phenocopies the *tcf3a*/*tcf3b* MO phenotype.

neurectoderm, and overexpression of *wnt8* expands posterior neural identity at the expense of anterior fates (Erter et al., 2001; Lekven et al., 2001). To test whether *nlk* inhibits expression of anterior neural markers during gastrulation, we fixed *nlk*- or *wnt8*-injected embryos at 90% epiboly and performed in situ hybridization using probes for *opl*, a telencephalic marker, and *tbx6*, a marker of ventrolateral mesoderm (Fig. 3). Like *wnt8*-injected embryos, *nlk*-injected embryos show a dramatic reduction of *opl* expression, indicative of a loss of anterior neural identity (compare the loss of *opl* in Fig. 3B,C with wild-type expression in 3A, indicated by arrowheads).

Phosphorylation of Tcf by Nlk specifically inhibits the DNA-binding ability of β-catenin/Tcf complexes, and not that of Tcf alone (Ishitani et al., 1999), suggesting that Nlk would only inhibit Tcf in the presence of β-catenin. To test whether the *nlk* overexpression phenotype is dependent on β-catenin stabilized by Wnt signaling, we co-injected morpholinos to two *wnt8* loci (hereafter referred to as *wnt8* ORF1 and ORF2) known to be required for proper AP patterning of the neuroectoderm (Lekven et al., 2001). We injected *nlk* RNA with either *wnt8* MOs or a control MO, and stained embryos at 90% epiboly with probes for *opl* and *tbx6*. We also scored for the presence of eyes at 24 hpf. Injection of *wnt8* MOs expands anterior neural fates, as shown by a posterior shift in the *opl* expression domain towards the margin (Fig. 3D, arrowhead; compare with wild type in 3A). Although *nlk* RNA/control MO embryos have dramatically reduced *opl* expression (Fig. 3E, arrowhead), co-injection of *wnt8* MOs with 200 pg of *nlk* RNA resulted in substantial rescue of *opl* expression (Fig. 3F, arrowhead; *opl* expression domain is shifted posteriorly, as with *wnt8* MOs alone, see Fig. 3D). The formation of eyes is also rescued at 24 hpf [Fig. 3H versus 3G, arrows; 15% of *nlk/wnt8* MO-injected embryos had small/reduced eyes (n=78) versus 56% of *nlk*/control MO injected embryos (n=52)]. We did not observe completely penetrant rescue of the *nlk* overexpression phenotype, possibly because of residual *wnt8* activity. This suggests that zebrafish *nlk*, as has been postulated for its mammalian counterparts, requires *wnt8*, and thus probably β-catenin, for full activity.

Morpholino antisense inhibition of *nlk*

To assess the function of endogenous *nlk*, we used morpholino antisense oligonucleotides to interfere with the splicing of *nlk* mRNA (Draper et al., 2001). We designed a morpholino to anneal to the splice donor site between exon 5 and intron 5 (see Fig. 4). Translation of the improperly spliced message would result in a truncated, probably non-functional, protein, with the 229 amino acids encoded by exons 1-5 appended to 19 non-

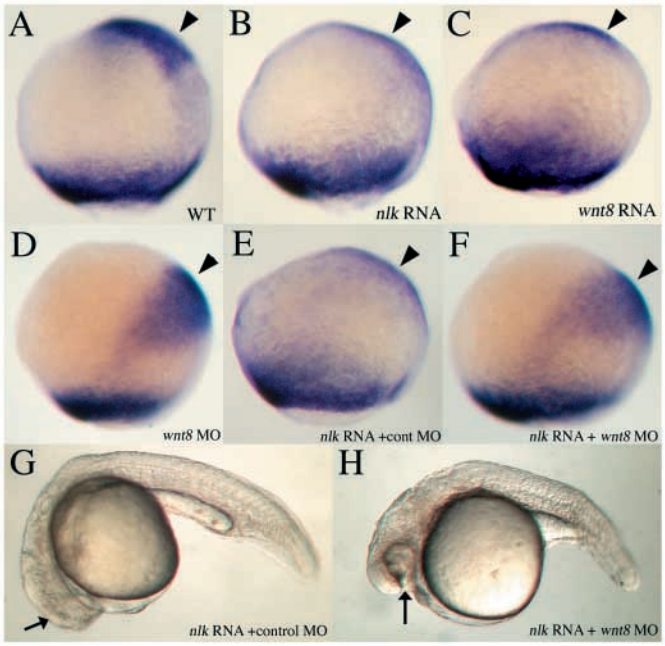

Fig. 3. *nlk* RNA represses anterior neural fate in a *wnt8*-dependent manner. (A-F) 90-95% epiboly, lateral view, dorsal to the right. Embryos are stained with a mix of *opl* and *tbx6* probes. Injection of 200 pg *nlk* RNA (B) or 10 pg *wnt8* RNA (C) represses expression of *opl* (arrowheads) in the prospective telencephalon, compared with wild type (A). Injection of 1 ng each of *wnt8* ORF1 and ORF2 morpholinos (MOs) causes a posterior shift of *opl* expression towards the margin (D, arrowhead). Co-injection of a control MO with *nlk* RNA has no effect on *opl* (E), whereas injection of *wnt8* MOs restores *opl* expression when co-injected with *nlk* RNA (F). (G,H) Twenty-four-hour embryos, lateral view, showing rescue of eyes in *nlk* RNA + *wnt8* MOs (G) versus *nlk* RNA + control MO (H).

conserved amino acids encoded by the 5′ end of intron 5, followed by a stop codon.

To test the efficacy of the *nlk* MO, we injected 1-3 ng *nlk* MO at the one-cell stage and isolated RNA from 24 hpf embryos (Fig. 4). We then performed RT-PCR using primers flanking intron 5 that are predicted to amplify a fragment of 233 bp from the spliced message and 320 bp from unspliced mRNA. We amplified only a band of approximately 230 bp from wild-type cDNA. By contrast, a larger product of approximately 320 bp was predominant in cDNA prepared from *nlk* MO-injected embryos. We confirmed that this larger band corresponds to the unspliced mRNA by DNA sequencing. Splicing of introns from unrelated genes is unaffected by injection of *nlk* MO, nor does injection of splice-blocking MO's targeted to other genes affect the splicing of *nlk* (data not shown). Although injection of higher doses of *nlk* MO caused a greater accumulation of unspliced mRNA (data not shown), it also led to an increase in common morpholino side affects, such as developmental delay. We therefore used a 1-3 ng dose of the splicing MO for the experiments reported here to minimize such effects. We also tested a translation-blocking *nlk* MO, which caused similar phenotypes (data not shown), but it was more toxic to embryos than the splicing MO. Confirming the specificity of the *nlk* MO phenotype, injection of *nlk* RNA was able to rescue *nlk* MO-injected embryos (see Fig. 6).

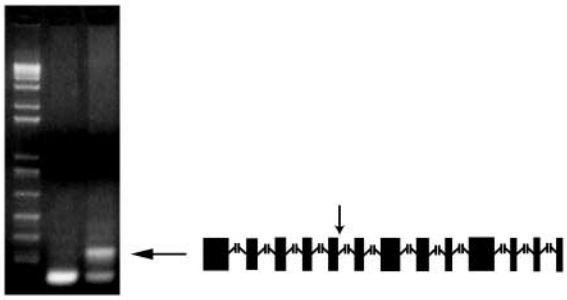

Fig. 4. *nlk* splice-blocking morpholino inhibits processing of *nlk* mRNA. Genomic structure of *nlk*, and RT-PCR analysis of the splicing of intron 5 in the *nlk* mRNA. Introns are not drawn to scale. Vertical arrow indicates intron/exon boundary between exon 5 and intron 5, targeted by *nlk* MO. Photo on left shows RT-PCR on RNA isolated from 24-hpf wild-type and *nlk* MO embryos. The wild-type sample contains only the 233 bp band predicted to result from correct splicing of intron 5. The horizontal arrow indicates the presence of a 320 bp band in the *nlk* MO sample, which was confirmed by sequencing to be the unspliced product.

nlk MO enhances the ventrolateral mesoderm defect of *wnt8* MO

The principle phenotypes observed in 24 hpf *nlk* morphants are a disorganization of the head and a moderately short tail (Fig. 5I, compare with wild type in 5C). Notably, *nlk* morphants did not have the enlarged forebrain and eyes characteristic of *wnt8* morphants (see Fig. 5F), suggesting that endogenous *nlk* does not play a role in posteriorization of the neurectoderm by *wnt8*, as suggested by the overexpression phenotype. To confirm this, we examined the expression of anterior neural markers during gastrulation in *nlk* morphants. Inhibition of *wnt8* by mutation or morpholino injection results in the posterior expansion of the expression domains of *otx2* and *opl* into the prospective posterior neural domain (Erter et al., 2001; Lekven et al., 2001). Injection of *nlk* MO had no effect on the expression patterns of these two genes, even when very high doses (10-15 ng) were used, nor did *nlk* MO injection enhance the phenotype of embryos injected with suboptimal doses of *wnt8* MOs (data not shown).

We did detect, however, a significant enhancement of the ventrolateral mesoderm defect observed in *wnt8* morphants (Fig. 5). In addition to its role in regulating AP polarity in the neurectoderm, *wnt8* is also required to limit the size of the dorsal organizer and for formation of ventrolateral mesoderm, which contributes to somitic mesoderm in the trunk and tail (Erter et al., 2001; Lekven et al., 2001). Both *wnt8* MO and *nlk* MO cause a modest reduction in the expression of *tbx6* in the ventrolateral margin, with a small increase in the width of the dorsal domain from which *tbx6* is excluded (Fig. 5D,G; compare to wild type in 5A; double-headed arrow indicates region of dorsal margin where *tbx6* is absent). At 24 hpf, both *nlk* MO embryos (Fig. 5I) and *wnt8* morphants (Fig. 5F) have a shortened tail compared with wild type (Fig. 5C), indicative of a mild defect in somitic mesoderm formation and consistent with the earlier reduction in *tbx6* expression. In situ hybridization at the 7-somite stage with a cocktail of probes containing *opl* (telencephalon), *pax2* (midbrain/hindbrain boundary, otic vesicles, pronephros), *krox20* (rhombomeres 3 and 5) and *myod* (somites) shows that *nlk* morphants express

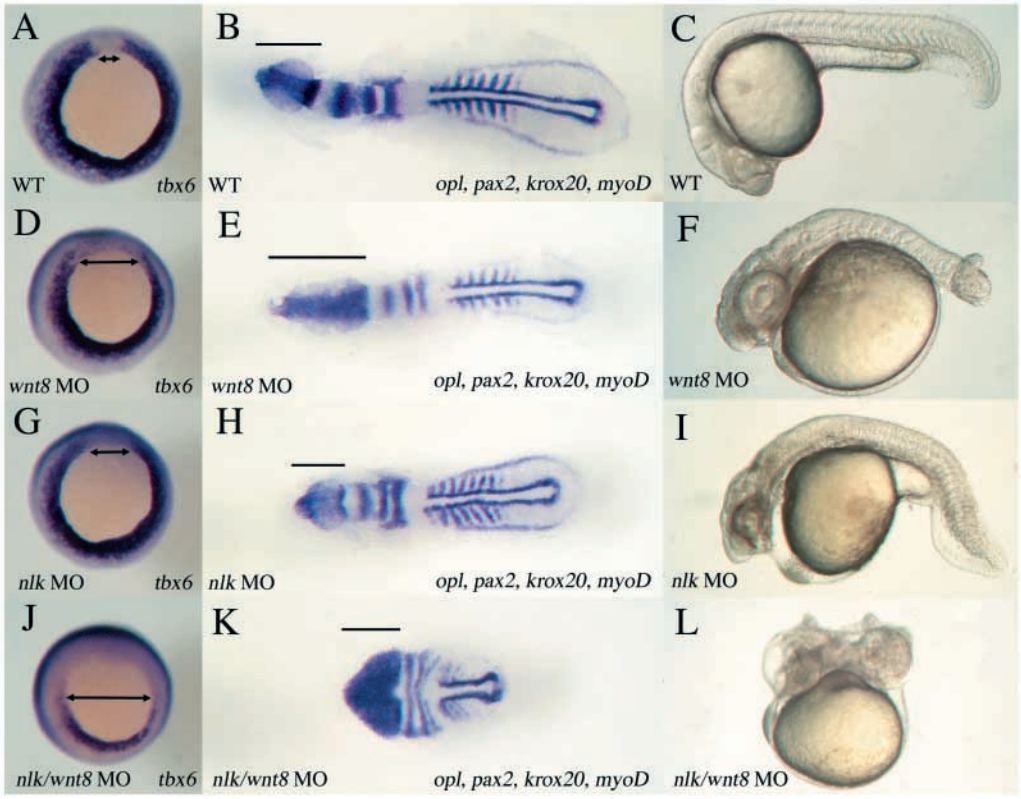

Fig. 5. *nlk* MO enhances the mesoderm defect of *wnt8* MOs. (A,B,C) Wild type, (D,E,F) *wnt8* MOs, (G,H,I) *nlk* MO and (J,K,L) *nlk* MO/*wnt8* MOs. A,D,G,J were stained for *tbx6* at 90% epiboly (vegetal view; dorsal to the top). B,E,H,K were stained with a mix of *opl*, *pax2*, *krox20* and *myod* at 6 to 7 somites (dorsal view; bars indicate the extent of *opl* expression). C,F,I,L were left to develop to 24 hpf (lateral view). *tbx6* expression is reduced in *wnt8* (D) and *nlk* (G) compared with wild type (A), whereas *nlk/wnt8* morphants have a dramatic reduction in *tbx6* (J; double-headed arrows indicate dorsal region of margin where *tbx6* is excluded). *wnt8* MO embryos have a greatly expanded *opl* domain, and a slightly wider notochord (E; notochord domain delineated by longitudinal stripes of adaxial *myod* expression), reflecting the defects in AP patenting of the neuroectoderm and in DV patterning in the mesoderm, characteristic of *wnt8* morphants. *nlk* morphants (H) are slightly shorter than wild type, but have no significant defects in neuroectoderm or mesoderm patterning. *nlk/wnt8* morphants (K) are dramatically shortened, with significantly broadened expression of neural markers, reflecting increased dorsalization of the embryos. Only a few trunk somites are formed, and tail formation does not occur. *nlk/wnt8* morphants at 24 hpf (L) are significantly shorter than wild type (C), *wnt8* MO (F) or *nlk* MO (I), and show a dorsal curvature of the tail characteristic of severely dorsalized embryos.

all of these markers normally [compare the *opl* domain, marked with a bar, in Fig. 5H with that in wild type in Fig. 5B, and with the expanded domain seen in *wnt8* MO-injected embryos (Fig. 5E)]. However, in *nlk/wnt8* MO embryos, we observe a significant enhancement of the mesoderm phenotype to a degree of severity that is never seen in *wnt8* or *nlk* morphants alone. When both *nlk* and *wnt8* function is blocked, *tbx6* expression is severely reduced in the ventrolateral margin, with a concomitant expansion of the axial domain lacking *tbx6* (Fig. 5J). The severity of the effect on *tbx6* expression resembles that seen in embryos homozygous for a chromosomal deficiency that completely removes the *wnt8* locus (Lekven et al., 2001). *nlk/wnt8* morphants have dramatically reduced trunk and tail mesoderm, and show a dramatically broadened expression of neural markers, reflecting the dorsalization of the embryos due to expansion of organizer fates (Fig. 5K). The most severely affected embryos completely lack the tail, and make only a few trunk somites (Fig. 5L). These data indicate that *nlk* functions with *wnt8* to specify ventrolateral mesoderm and to limit the size of the dorsal organizer.

wnt8 likely functions through *lef1* to specify ventrolateral mesoderm, as *lef1* morphants also show decreased *tbx6* expression during gastrulation (Dorsky et al., 2002). In contrast to *tcf3a* and *tcf3b*, *lef1* appears to function predominantly as an activator of Wnt target genes (Kengaku et al., 1998; Merrill et al., 2001). We tested whether *nlk* and *lef1* cooperate to activate *tbx6* by co-injecting both morpholinos and examining *tbx6* expression (Fig. 6). When *nlk* MO is injected at a low dose (0.6 ng), no effect on *tbx6* is seen at 60% epiboly (Fig. 6B, compare with wild type in 6A). *lef1* MO, as previously reported, reduces *tbx6* expression (Fig. 6C). When 0.6 ng *nlk* MO is co-injected with *lef1* MO, *tbx6* expression is almost completely eliminated (Fig. 6D). It has recently been reported that *tcf3a/tcf3b* double morphants have elevated levels of *lef1* transcripts during early gastrulation, suggesting that one role of *tcf3a* and *tcf3b* is to negatively regulate *lef1* expression (Dorsky et al., 2003). Thus, one explanation for the synergy between *nlk* and *lef1* could be that *nlk* is required for relieving *tcf3*-mediated repression of *lef1* transcription. To test this hypothesis, we examined *lef1* expression in *nlk* MO-injected embryos. At shield stage, *lef1* expression is reduced in *nlk* morphants compared with wild-type embryos (compare Fig. 6F with 6E). If *nlk* activates *lef1* expression by inhibiting *tcf3a* and *tcf3b*, then injection of *tcf3a* and *tcf3b* MOs should rescue *lef1* expression in *nlk* morphants. Indeed, we found that *nlk/tcf3a/tcf3b* MO embryos (Fig. 6H), like *tcf3a/tcf3b* morphants (Fig. 6G), showed significantly elevated *lef1* expression compared with wild type, suggesting that *nlk* is not directly required for *lef1* transcription, but functions indirectly by modulating *tcf3a/tcf3b* activity. Expression of *tcf3a* and *tcf3b* is unaffected in *nlk* morphants (data not shown), indicating that the interaction between *nlk* and *tcf3a/3b* is not due to upregulation of *tcf3a/3b* transcription in the absence of *nlk*.

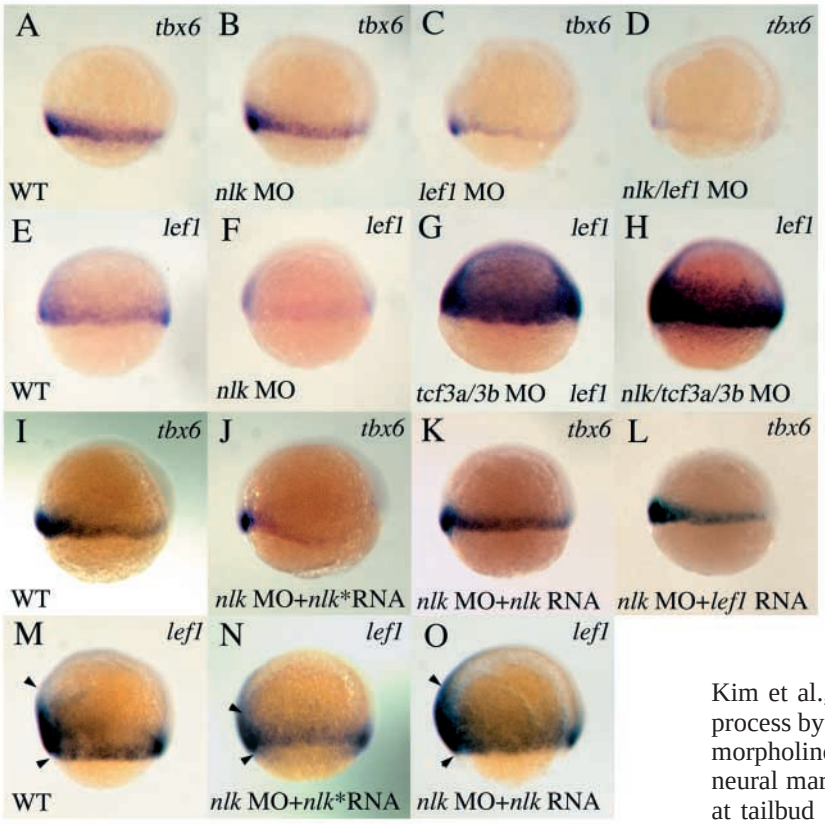

Fig. 6. *nlk* and *lef1* cooperatively regulate *tbx6*, and *nlk* regulates *lef1* expression. (A-D) *tbx6* expression at 60% epiboly, lateral view, dorsal to the right. A low dose (0.6 ng) of *nlk* MO has no effect on *tbx6* expression (B, compare with wild type in A). 1 ng *lef1* MO reduces *tbx6* expression (C), and this effect is enhanced by co-injection of 0.6 ng *nlk* MO (D). (E-H) Expression of *lef1* at shield stage, lateral view, dorsal to the right. *lef1* is expressed at the margin in wild type (E), but is reduced in *nlk* MO (F). *lef1* expression is dramatically elevated in *tcf3a/tcf3b* morphants (G) and in *nlk/tcf3a/tcf3b* MO embryos (H). (I-L) *nlk* or *lef1* RNA rescues *tbx6* expression in *nlk* morphants. *nlk** RNA refers to the C387Y mutant. Co-injection of 200pg *nlk* RNA (K), but not *nlk** RNA (J), restores *tbx6* expression to levels similar to wild type (I). 100pg *lef1* RNA (L) also rescues *nlk* morphants. Similarly, *nlk* RNA rescues normal *lef1* expression (O, compare with wild type in M; arrowheads delineate the expression domain), whereas *nlk** RNA (N) does not.

To confirm that these phenotypes were due to loss of *nlk* function, we attempted to rescue the reduction of *tbx6* and *lef1* expression in *nlk* morphants by co-injecting *nlk* RNA. As a control RNA, we co-injected *nlk* (C387Y) RNA (shown as *nlk** RNA in Fig. 6). *nlk* RNA significantly rescues the reduction in *tbx6* expression (compare Fig. 6K with 6J) induced by *nlk* MO injection [80% show wild-type levels of expression at 60% epiboly (n=65) versus 29% (n=63) when *nlk* (C387Y) RNA was co-injected). *lef1* RNA was also able to restore normal *tbx6* expression in *nlk* MO embryos (Fig. 6L; 77% show wild-type expression, n=60), further suggesting that the reduction in *tbx6* expression in *nlk* morphants is due to a reduction in *lef1*. *nlk* RNA was able to restore normal *lef1* expression in a significant fraction of *nlk* morphants. Although only 27% (n=62) of *nlk* MO/*nlk* (C387Y) RNA-injected embryos had wild-type levels of *lef1* at 60-70% epiboly (compare Fig. 6N with wild type in 6M), 70% (n=43) of *nlk* MO/*nlk* RNA-injected embryos (Fig. 6O) had normal levels of *lef1*. Taken together, these results show that *nlk* MO specifically interferes with *nlk* function, and that *nlk* is required for normal *lef1* expression and subsequent ventrolateral mesoderm formation.

nlk morphants are defective in later aspects of AP brain patterning

Wnt signaling late in gastrulation has been proposed to regulate regional identity within the anterior neural plate, apart from the earlier action of *wnt8* ORF1 and ORF2 (Heisenberg et al., 2001; Houart et al., 2002; Houart et al., 1998; Kim et al., 2002; van de Water et al., 2001). Knockdown of either *wnt8b* or *fz8a* results in a reduction in the expression of markers in the midbrain and posterior diencephalon, suggesting that these two genes play key roles in promoting development of these regions of the brain (Houart et al., 2002; Kim et al., 2002). We tested whether *nlk* plays a role in this process by injecting embryos with *nlk* MO, *wnt8b* MO, or both morpholinos together, and staining embryos with several neural markers (Fig. 7). In one experiment, we fixed embryos at tailbud stage and probed with a cocktail of *opl*, *pax2* and *tbx6* to mark the telencephalon, MHB and margin (Fig. 7A-C), or with *en2* to mark the prospective MHB and midbrain (Fig. 7D-F). We observed no changes in *opl* expression in *wnt8b* MO (Fig. 7B) or *nlk* MO (Fig. 7C) embryos, confirming published results for *wnt8b* MO (Kim et al., 2002) and indicating that *wnt8*-dependent posteriorization was occurring normally. *pax2* expression was normal in *wnt8b* morphants, but reduced in *nlk* MO embryos, similar to what is observed in *fz8a* MO embryos (Kim et al., 2002). *en2* is substantially reduced in most *wnt8b* morphants (Fig. 7E, compare with control in 7D), as previously reported, and is eliminated in most *nlk* MO embryos (Fig. 7F). When we examined *en2* expression at the 7-somite stage, *en2* was present but at a much reduced level in *wnt8b*MO- (76%; n=45; Fig. 7H) or *nlk* MO (81%; n=42; Fig. 7I)-injected embryos. Co-injection of a high dose (1 ng each) of both morpholinos does not result in a stronger phenotype, but does increase the penetrance somewhat (95%; n=17). When low doses (0.5 ng) are injected, both *nlk* MO and *wnt8b*MO still cause a reduction of *en2* staining at the 7-somite stage, but at a lower penetrance [48% (n=27) and 51% (n=31), respectively]. Co-injection of both MOs at the lower doses results in a significant increase in the penetrance of the *en2* phenotype (91%; n=35), suggesting that *nlk* and *wnt8b* are functioning together to regulate *en2* expression.

Injection of *wnt8b* morpholinos has also been reported to cause a modest reduction in *pax6* expression in the posterior diencephalon during early somitogenesis (Kim et al., 2002). When we examined *pax6* expression at the 7-somite stage in *wnt8b*MO- or *nlk* MO-injected embryos, we found that the diencephalic domain of *pax6* expression was reduced in *nlk* MO-injected embryos (Fig. 7L, compare with control, 7J), although we did not observe a significant reduction in *wnt8b*MO (Fig. 7K) embryos. Kim et al. (Kim et al., 2002)

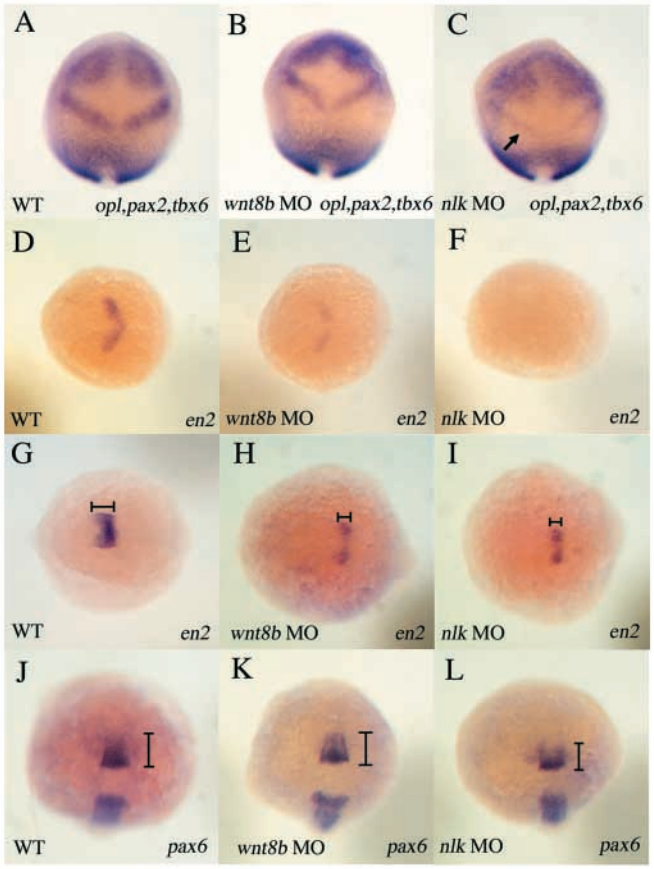

Fig. 7. *nlk* MO affects expression of MHB and diencephalon markers. Embryos were injected with *nlk* or *wnt8b* MOs. At bud stage, embryos were stained with either a mix of *opl*, *pax2* and *tbx6* (A,B,C; dorsal view, anterior to top), or with *en2* (D,E,F; dorsal view, anterior to left). At 7 somites, embryos were stained with either *en2* (G,H,I; dorsal view, anterior to left) or *pax6* (J,K,L; dorsal view, anterior to top). Although expression of *opl* and *pax2* are unaffected in *wnt8b* morphants (B) compared with wild type (A), *nlk* morphants have a slight reduction in *pax2* expression (C; arrow). *en2* expression is reduced in *wnt8b* MO (E), and is eliminated in *nlk* MO (F) compared with wild type (D). At 7 somites, *en2* is expressed in the MHB and midbrain (G). Expression is substantially reduced in both *wnt8b* and *nlk* morphants (H,I; brackets delineate expression domain). *pax6* expression is unchanged in *wnt8b* MO (K), but is reduced slightly in *nlk* MO (L; brackets indicate AP extent of expression domain).

reported only a very mild reduction in the *pax6* domain in *wnt8b* morphants, but *fz8a* morphants showed a more severe reduction, similar to what we observe in *nlk* MO embryos. Taken together, our data implicate *nlk* in regulating AP patterning in the neural plate, possibly in conjunction with *wnt8b* and *fz8a*.

nlk interacts with non-canonical Wnt signals

The data above indicate that *nlk* can function with canonical Wnts in regulating aspects of mesoderm and neurectoderm development. Recently published work using mammalian cell culture supports a potential role for Nlk as a downstream effector of non-canonical Wnts such as Wnt5a (Ishitani et al., 2003a). In vertebrates, non-canonical Wnts, together with homologs of *Drosophila* planar cell polarity (PCP) signaling pathway components such as *strabismus* and *prickle*, regulate convergence/extension movements during gastrulation (reviewed by Tada et al., 2002; Veeman et al., 2003). As *nemo* mutants in *Drosophila* exhibit some defects in PCP signaling, it is possible that the cell culture data describes a conserved role for Nlk proteins in non-canonical Wnt signaling (Choi and Benzer, 1994; Verheyen et al., 2001). Therefore, we attempted to detect genetic interactions between *nlk* and non-canonical Wnt signaling in zebrafish.

In zebrafish, mutations in two non-canonical Wnts, *pipetail* (*ppt*)/*wnt5* and *silberblick* (*slb*)/*wnt11*, have been characterized. *ppt*/*wnt5* embryos are defective in tail extension, whereas *slb*/*wnt11* mutations cause partial cyclopia due to a defect in migration of the anterior axial mesoderm, the prechordal plate (Heisenberg and Nusslein-Volhard, 1997; Heisenberg et al., 2000; Kilian et al., 2003; Rauch et al., 1997; Ulrich et al., 2003). To test for genetic interactions between *nlk* and *ppt*/*wnt5*, we injected *nlk* MO into embryos from a cross of *ppt* heterozygotes. *nlk* MO/*ppt* embryos display only an additive phenotype, with a moderately more severe tail defect (data not shown).

By contrast, we observe a strong interaction between *nlk* and *wnt11*/*slb*. We quantified the severity of the phenotype by calculating the Cyclopia Index (CI) (Marlow et al., 1998) (see Fig. 8). Injection of 0.5 ng *wnt11* MO causes a mild phenotype, with the large majority of embryos being either unaffected or having slightly more closely set eyes (CI=1.59). *nlk* MO has no cyclopia phenotype on its own, but strongly enhances the *wnt11* MO phenotype, resulting in many embryos with complete eye fusion (CI=3.98). As a control, we saw no effect on the *wnt11* MO phenotype upon co-injection of *wnt8* ORF1 MO (CI=1.54 versus 1.59 in *wnt11* MO alone). We directly analyzed migration of the prechordal plate by fixing embryos at 95-100% epiboly and staining with probes for *tbx6* (to mark the margin) and *gsc* (to mark the prechordal plate). Although all *nlk* MO (n=45), and most *wnt11* MO (85%, n=41) embryos showed normal migration of the prechordal plate to near the animal pole (Fig. 8C,D, arrowheads; compare with wild type in B), most *nlk/wnt11* MO embryos showed a dramatic defect in migration of the prechordal plate (Fig. 8E). This effect of *nlk* MO on prechordal plate migration is specific to *wnt11*, as co-injection of *nlk* MO does not enhance the mild cyclopia induced by injection of low doses of *strabismus/trilobite* MO (Fig. 8), nor does it enhance the phenotype of *knypek/glypican4* mutants (data not shown), which very rarely exhibit partial cyclopia, but which do strongly enhance the cyclopic phenotype of both *wnt11* and *strabismus* mutants (Henry et al., 2000; Jessen et al., 2002; Park and Moon, 2002; Sepich et al., 2000; Topczewski et al., 2001).

Previous work has indicated that although *wnt8* ORF1 and ORF2 function redundantly in mesoderm and neurectoderm patterning, they may possess different signaling capabilities (Lekven et al., 2001). Whereas *wnt8* ORF1 seems to signal strictly canonically, in some overexpression assays *wnt8* ORF2 behaves similarly to non-canonical Wnts. We therefore tested whether *wnt8* ORF2 interacted with *wnt11*. Injection of *wnt8* ORF2 MO significantly enhanced the phenotype of *wnt11* morphants (CI=2.61), suggesting that *wnt8* ORF2 may have a non-canonical signaling role. Like *nlk*, knockdown of *wnt8*

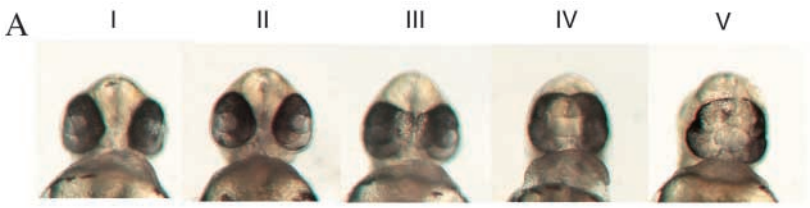

Morphotype	I	II	III	IV	V	Index	N
nlk MO	173	0	0	0	0	1.00	173
*wnt11*MO	45	30	3	0	3	1.59	81
nlk MO/*wnt11*MO	14	12	0	18	64	3.98	108
wnt8.1 MO	141	0	0	0	0	1.00	141
wnt8.1 MO/*wnt11*MO	74	42	10	0	2	1.54	128
strabismus MO	66	13	3	0	0	1.23	82
nlk MO/*strabismus* MO	59	13	5	0	0	1.23	125
wnt8.1/*strabismus* MO	38	10	1	2	0	1.35	51
wnt8.2 MO	98	0	0	0	0	1.00	98
wnt8.2 MO/*nlk* MO	110	0	0	0	0	1.00	110
wnt8.2 MO/*wnt11* MO	36	34	39	34	13	2.61	146
wnt8.2 MO/*strabismus* MO	57	10	0	0	0	1.15	67

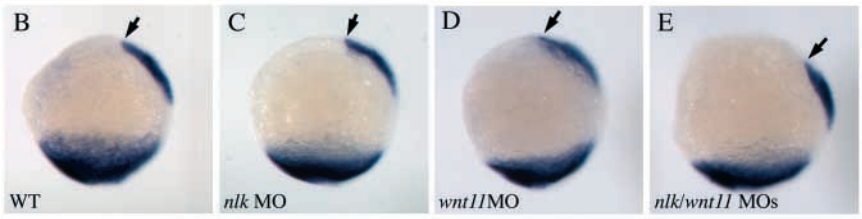

Fig. 8. *nlk* and *wnt8* ORF2 MOs enhance the phenotype of *wnt11*. Morpholinos were injected in the combinations listed in the table. *wnt8.1* refers to *wnt8* ORF1 and *wnt8.2* refers to *wnt8* ORF2. *Wnt11* and *strabismus* morpholinos were injected at a concentration of 0.5 ng/nl, whereas *nlk*, *wnt8* ORF1 and *wnt8* ORF2 MOs were injected at a concentration of 1 ng/nl. (A) Embryos were scored at 48 hours and placed into five phenotypic classes based on the severity of the cyclopia phenotype (Classes I-V, according to Marlow et al.), and the Cyclopia Index (Marlow et al., 1998) was calculated for each experiment. (B-E) Embryos were injected with *nlk*, *wnt11*, or both morpholinos, fixed at 100% epiboly, and stained with probes for *tbx6* and *gsc*. The anterior extent of the *gsc* domain is marked with an arrowhead.

ORF2 did not enhance the weak cyclopia in *tri/strabismus* morphants. Although *nlk* and *wnt8* ORF2 MO both enhance *wnt11* loss of function, knocking out *nlk* and ORF2 together does not reveal any redundancy between the two genes (CI=1.00). Although our data do not definitively place *nlk* downstream of a non-canonical Wnt, they clearly indicate that *nlk* genetically interacts with *wnt11/slb* to regulate cell movements during gastrulation, possibly in conjunction with *wnt8* ORF2.

Discussion

Zebrafish *nlk* interacts with both canonical and non-canonical Wnt pathways

Our results support a role for *nlk* in the activation of Wnt targets during zebrafish embryogenesis. Overexpressed *nlk* downregulates two *tcf3* homologs, *tcf3a* and *tcf3b*, that repress activation of Wnt target genes during neural patterning. This functional interaction with Tcf3 homologs requires *wnt8* signaling, and thus probably β-catenin, consistent with previous data indicating that Nlk specifically interferes with the DNA-binding ability of β-catenin/Tcf complexes, not that of Tcf alone. Interference with endogenous *nlk* function reveals important roles in two processes that are regulated by canonical Wnts, mesoderm patterning by *wnt8*, and patterning of midbrain and forebrain by *wnt8b*. As loss of *nlk* enhances or phenocopies loss of function of these two Wnts, we conclude that *nlk* functions as an activator of some canonical Wnt targets in zebrafish. *nlk* also interacts, directly or indirectly, with non-canonical Wnt pathways, as inhibition of *nlk* strongly enhances convergent extension phenotypes associated with loss of *wnt11* function. We also uncover a role for an unusual *wnt8* homolog, *wnt8* ORF2, in regulating cell movements during gastrulation.

nlk inhibits *tcf3a* and *tcf3b*, not *lef1*

The interplay between caudalizing *wnt8* and rostrally localized *tcf3* homologs functioning as inhibitors of Wnt signaling helps establish AP polarity within the neural plate. Overexpression of *nlk* in zebrafish phenocopies the effects of ectopic *wnt8* signaling on AP patterning, and enhances the phenotype associated with loss of *tcf3* function. In light of the well-established ability of Nlk homologs in other species to phosphorylate Tcfs and inhibit the DNA binding ability of β-catenin/Tcf complexes, we suggest that Nlk and β-catenin can function together to derepress genes inhibited by Tcf3a and Tcf3b. This provides the first evidence in vertebrates that Nlk can function as a positive regulator of canonical Wnt target genes.

Mouse Nlk has been shown to directly interact with both mammalian Lef1 and Tcf4, as well as *Xenopus* Tcf3 (Ishitani et al., 2003b; Ishitani et al., 1999; Meneghini et al., 1999). Mutational analysis has demonstrated that Nlk phosphorylates conserved serine and threonine residues on Lef1 and Tcf4, and that these residues are required for Nlk to inhibit the DNA-binding ability of Tcf/β-catenin complexes (Ishitani et al., 2003b). Zebrafish *tcf3a*, *tcf3b* and *lef1* all possess serine or threonine residues at analogous sites to their mammalian homologs, suggesting that they are all potential substrates for *nlk*. Interestingly, overexpression of zebrafish *nlk* only affects AP patterning in the neurectoderm, consistent with an inhibition of only *tcf3a* and *tcf3b*, not of *lef1*. Also, overexpression of *nlk* does not cause ventralization in either zebrafish or *Xenopus* (J. Waxman, unpublished), suggesting that *nlk* does not interact with a (as yet unknown) Tcf/Lef protein required for transducing maternal β-catenin signaling. By contrast, mouse Nlk can block dorsal axis formation in *Xenopus* (Ishitani et al., 1999), and can block formation of dorsal mesoderm when injected into zebrafish (data not shown), suggesting that it can inhibit maternal β-catenin signaling. Although little is known regarding which regions of

Nlk are important for interaction with β-catenin or Tcf/Lef proteins, it is possible that the substantial differences between mammalian and zebrafish *nlk* over the first 90-100 amino acids could contribute to the differences in phenotypes when overexpressed. In early zebrafish development, *nlk* seems to interact specifically with two Tcf3 genes known to play a role in the repression of Wnt target genes, but not with *lef1*, which has been proposed to function primarily as an activator.

nlk morphants are defective in canonical Wnt signaling

Mutational analyses in *Drosophila* and in mice have been inconclusive in distinguishing whether Nlk functions as an activator or an inhibitor of the Wnt pathway. For example, *nemo* mutant flies show, among other phenotypes, a variable segment polarity phenotype that can include both excess naked cuticle, indicative of excess *wingless* (*wg*)/Wnt signaling, and loss of denticle diversity, which is suggestive of a reduction of *wg* signaling (Mirkovic et al., 2002; Verheyen et al., 2001). Similarly, the mouse knockout causes a pleiotropic phenotype that may or may not reflect an underlying role in the regulation of Wnt signaling (Kortenjann et al., 2001a).

Our loss-of-function studies support a role for *nlk* in regulating canonical Wnt signaling. The enhancement of *wnt8* and *lef1* loss-of-function phenotypes suggests that *nlk* is functioning as an activator of Wnt targets in mesoderm patterning. As *nlk* is required for *lef1* expression in the presence of *tcf3*, our data support a model in which *nlk* relieves *tcf3*-mediated repression of *lef1* transcription during gastrulation. β-catenin stabilized by *wnt8* could then interact with Lef1 to activate *tbx6* and other genes.

Our observation that *nlk* MO causes defects in *en2* and *pax6* expression similar to those seen in *wnt8b* and *fz8a* morphants suggests that *nlk* may be functioning in this later AP patterning event. A simple hypothesis is that *nlk* relieves the repression of *wnt8b* targets by *tcf3a* and/or *tcf3b*. Supporting a possible role for *tcf3a* in regulating *wnt8b* signaling, injection of lower doses of *tcf3a* MO (0.5 ng) or *nlk* RNA (100 pg) results in embryos with normal *pax2* expression and an expanded *pax6* domain, as would be expected from ectopic *wnt8b* signaling (Kim et al., 2002) (and data not shown). This phenotype indicates that *tcf3a* may act to limit *wnt8b* signaling within the rostral neurectoderm, and suggests that *nlk* could function in *wnt8b*-mediated patterning by inhibiting *tcf3a*.

Given that overexpression of *nlk* expands posterior neural fates in a *wnt8*-dependent manner, we were somewhat surprised that we did not observe any affects of *nlk* MO on the expression of neural genes known to be regulated by *wnt8*, such as *opl*. Although we note that a comprehensive search of sequenced mammalian and invertebrate genomes indicates that only one Nlk homolog is present, an ancient gene duplication event in the ancestry of teleost fish has led to the presence of multiple copies of many genes that are present only once in tetrapods, raising the possibility that additional Nlk homolog(s) in zebrafish could be functioning in this process (Kortenjann et al., 2001b; Taylor et al., 2001).

nlk and *wnt8* ORF2 interact with non-canonical Wnt11 signaling

The strong enhancement of the *slb/wnt11* phenotype by *nlk* MO indicates that *nlk* has an important role in regulating cell movements during gastrulation. Our data do not necessarily place *nlk* downstream of a non-canonical Wnt, as has been demonstrated in cell culture with mouse Nlk and Wnt5a. Although components of non-canonical Wnt pathways are clearly important for controlling cell movements, canonical Wnt signaling can also play a role. For example, in zebrafish, maternal β-catenin signaling is known to activate Stat3, which is required for normal convergence/extension movements (Yamashita et al., 2002). Maternal β-catenin signaling has also been shown to regulate gastrulation movements in *Xenopus*, probably through activation of *Xenopus nodal-related 3* (*Xnr3*) (Kuhl et al., 2001). Thus, the observed interaction between *nlk* and *wnt11* could reflect a defect in the regulation of a canonical Wnt target caused by loss of *nlk*, particularly in light of the observation that *nlk* morphants do not show any obvious convergence-extension defects.

Given the potent affects on cell proliferation and fate specification by Wnts, it is essential to restrict activation of Wnt target genes to only the appropriate time and place within an organism. It is likely, then, that many Wnt targets are actively repressed in the absence of Wnt ligand, and a significant function of Wnts in these contexts is to derepress them, permitting activation by other factors. Nlk is an important component of the mechanism by which some Wnt targets are activated in *C. elegans*, and this activity appears to be conserved in zebrafish.

We thank Rich Dorsky for providing the *lef1* and *tcf3b* morpholinos and the *lef1* plasmid; Thuy Tran for fish care; members of the Moon Laboratory for comments on this manuscript; and Josh Waxman for *Xenopus* injections. C.J.T. is an Associate, and R.T.M. an Investigator of the HHMI, which supported this research.

References

Behrens, J. (2000). Cross-regulation of the Wnt signalling pathway: a role of MAP kinases. *J. Cell Sci.* **113**, 911-919.

Cadigan, K. M. and Nusse, R. (1997). Wnt signaling: a common theme in animal development. *Genes Dev.* **11**, 3286-3305.

Choi, K. W. and Benzer, S. (1994). Rotation of photoreceptor clusters in the developing Drosophila eye requires the nemo gene. *Cell* **78**, 125-136.

Dorsky, R. I., Sheldahl, L. C. and Moon, R. T. (2002). A transgenic Lef1/beta-catenin-dependent reporter is expressed in spatially restricted domains throughout zebrafish development. *Dev. Biol.* **241**, 229-237.

Dorsky, R. I., Itoh, M., Moon, R. T. and Chitnis, A. (2003). Two tcf3 genes cooperate to pattern the zebrafish brain. *Development* **130**, 1937-1947.

Erter, C. E., Wilm, T. P., Basler, N., Wright, C. V. and Solnica-Krezel, L. (2001). Wnt8 is required in lateral mesendodermal precursors for neural posteriorization in vivo. *Development* **128**, 3571-3583.

Fekany-Lee, K., Gonzalez, E., Miller-Bertoglio, V. and Solnica-Krezel, L. (2000). The homeobox gene bozozok promotes anterior neuroectoderm formation in zebrafish through negative regulation of BMP2/4 and Wnt pathways. *Development* **127**, 2333-2345.

Heisenberg, C. P. and Nusslein-Volhard, C. (1997). The function of silberblick in the positioning of the eye anlage in the zebrafish embryo. *Dev. Biol.* **184**, 85-94.

Heisenberg, C. P., Tada, M., Rauch, G. J., Saude, L., Concha, M. L., Geisler, R., Stemple, D. L., Smith, J. C. and Wilson, S. W. (2000). Silberblick/Wnt11 mediates convergent extension movements during zebrafish gastrulation. *Nature* **405**, 76-81.

Heisenberg, C. P., Houart, C., Take-Uchi, M., Rauch, G. J., Young, N., Coutinho, P., Masai, I., Caneparo, L., Concha, M. L., Geisler, R. et al. (2001). A mutation in the Gsk3-binding domain of zebrafish Masterblind/Axin1 leads to a fate transformation of telencephalon and eyes to diencephalon. *Genes Dev.* **15**, 1427-1434.

Henry, C. A., Hall, L. A., Burr Hille, M., Solnica-Krezel, L. and Cooper, M. S. (2000). Somites in zebrafish doubly mutant for knypek and trilobite

form without internal mesenchymal cells or compaction. *Curr. Biol.* **10**, 1063-1066.

Houart, C., Westerfield, M. and Wilson, S. W. (1998). A small population of anterior cells patterns the forebrain during zebrafish gastrulation. *Nature* **391**, 788-792.

Houart, C., Caneparo, L., Heisenberg, C., Barth, K., Take-Uchi, M. and Wilson, S. (2002). Establishment of the telencephalon during gastrulation by local antagonism of Wnt signaling. *Neuron* **35**, 255-265.

Hyodo-Miura, J., Urushiyama, S., Nagai, S., Nishita, M., Ueno, N. and Shibuya, H. (2002). Involvement of NLK and Sox11 in neural induction in Xenopus development. *Genes Cells* **7**, 487-496.

Ishitani, T., Ninomiya-Tsuji, J., Nagai, S., Nishita, M., Meneghini, M., Barker, N., Waterman, M., Bowerman, B., Clevers, H., Shibuya, H. et al. (1999). The TAK1-NLK-MAPK-related pathway antagonizes signalling between beta-catenin and transcription factor TCF. *Nature* **399**, 798-802.

Ishitani, T., Kishida, S., Hyodo-Miura, J., Ueno, N., Yasuda, J., Waterman, M., Shibuya, H., Moon, R. T., Ninomiya-Tsuji, J. and Matsumoto, K. (2003a). The TAK1-NLK mitogen-activated protein kinase cascade functions in the Wnt-5a/Ca(2+) pathway to antagonize Wnt/beta-catenin signaling. *Mol. Cell. Biol.* **23**, 131-139.

Ishitani, T., Ninomiya-Tsuji, J. and Matsumoto, K. (2003b). Regulation of lymphoid enhancer factor 1/T-cell factor by mitogen-activated protein kinase-related Nemo-like kinase-dependent phosphorylation in Wnt/beta-catenin signaling. *Mol. Cell. Biol.* **23**, 1379-1389.

Jessen, J. R., Topczewski, J., Bingham, S., Sepich, D. S., Marlow, F., Chandrasekhar, A. and Solnica-Krezel, L. (2002). Zebrafish trilobite identifies new roles for Strabismus in gastrulation and neuronal movements. *Nat. Cell Biol.* **4**, 610-615.

Kelly, G. M., Greenstein, P., Erezyilmaz, D. F. and Moon, R. T. (1995). Zebrafish wnt8 and wnt8b share a common activity but are involved in distinct developmental pathways. *Development* **121**, 1787-1799.

Kengaku, M., Capdevila, J., Rodriguez-Esteban, C., De La Pena, J., Johnson, R. L., Belmonte, J. C. and Tabin, C. J. (1998). Distinct WNT pathways regulating AER formation and dorsoventral polarity in the chick limb bud. *Science* **280**, 1274-1277.

Kilian, B., Mansukoski, H., Barbosa, F. C., Ulrich, F., Tada, M. and Heisenberg, C. P. (2003). The role of Ppt/Wnt5 in regulating cell shape and movement during zebrafish gastrulation. *Mech. Dev.* **120**, 467-476.

Kim, C. H., Oda, T., Itoh, M., Jiang, D., Artinger, K. B., Chandrasekharappa, S. C., Driever, W. and Chitnis, A. B. (2000). Repressor activity of Headless/Tcf3 is essential for vertebrate head formation. *Nature* **407**, 913-916.

Kim, S. H., Shin, J., Park, H. C., Yeo, S. Y., Hong, S. K., Han, S., Rhee, M., Kim, C. H., Chitnis, A. B. and Huh, T. L. (2002). Specification of an anterior neuroectoderm patterning by Frizzled8a-mediated Wnt8b signalling during late gastrulation in zebrafish. *Development* **129**, 4443-4455.

Kortenjann, M., Nehls, M., Smith, A. J., Carsetti, R., Schuler, J., Kohler, G. and Boehm, T. (2001a). Abnormal bone marrow stroma in mice deficient for nemo-like kinase, Nlk. *Eur. J. Immunol.* **31**, 3580-3587.

Kortenjann, M., Wehrle, C., Nehls, M. C. and Boehm, T. (2001b). Only one nemo-like kinase gene homologue in invertebrate and mammalian genomes. *Gene* **278**, 161-165.

Kuhl, M., Geis, K., Sheldahl, L. C., Pukrop, T., Moon, R. T. and Wedlich, D. (2001). Antagonistic regulation of convergent extension movements in Xenopus by Wnt/beta-catenin and Wnt/Ca2+ signaling. *Mech. Dev.* **106**, 61-76.

Lekven, A. C., Thorpe, C. J., Waxman, J. S. and Moon, R. T. (2001). Zebrafish wnt8 encodes two Wnt8 proteins on a bicistronic transcript and is required for mesoderm and neurectoderm patterning. *Dev. Cell* **1**, 103-114.

Lele, Z., Bakkers, J. and Hammerschmidt, M. (2001). Morpholino phenocopies of the swirl, snailhouse, somitabun, minifin, silberblick, and pipetail mutations. *Genesis* **30**, 190-194.

Maduro, M. F., Meneghini, M. D., Bowerman, B., Broitman-Maduro, G. and Rothman, J. H. (2001). Restriction of mesendoderm to a single blastomere by the combined action of SKN-1 and a GSK-3beta homolog is mediated by MED-1 and -2 in C. elegans. *Mol. Cell* **7**, 475-485.

Marlow, F., Zwartkruis, F., Malicki, J., Neuhauss, S. C., Abbas, L., Weaver, M., Driever, W. and Solnica-Krezel, L. (1998). Functional interactions of genes mediating convergent extension, knypek and trilobite, during the partitioning of the eye primordium in zebrafish. *Dev. Biol.* **203**, 382-399.

Meneghini, M. D., Ishitani, T., Carter, J. C., Hisamoto, N., Ninomiya-Tsuji, J., Thorpe, C. J., Hamill, D. R., Matsumoto, K. and Bowerman, B. (1999). MAP kinase and Wnt pathways converge to downregulate an HMG-domain repressor in Caenorhabditis elegans. *Nature* **399**, 793-797.

Merrill, B. J., Gat, U., DasGupta, R. and Fuchs, E. (2001). Tcf3 and Lef1 regulate lineage differentiation of multipotent stem cells in skin. *Genes Dev.* **15**, 1688-1705.

Mirkovic, I., Charish, K., Gorski, S. M., McKnight, K. and Verheyen, E. M. (2002). Drosophila nemo is an essential gene involved in the regulation of programmed cell death. *Mech. Dev.* **119**, 9-20.

Nasevicius, A. and Ekker, S. C. (2000). Effective targeted gene 'knockdown' in zebrafish. *Nat. Genet.* **26**, 216-220.

Oxtoby, E. and Jowett, T. (1993). Cloning of the zebrafish krox-20 gene (krx-20) and its expression during hindbrain development. *Nucl. Acids Res.* **21**, 1087-1095.

Park, M. and Moon, R. T. (2002). The planar cell-polarity gene stbm regulates cell behaviour and cell fate in vertebrate embryos. *Nat. Cell Biol.* **4**, 20-25.

Peifer, M. and Polakis, P. (2000). Wnt signaling in oncogenesis and embryogenesis – a look outside the nucleus. *Science* **287**, 1606-1609.

Rauch, G. J., Hammerschmidt, M., Blader, P., Schauerte, H. E., Strahle, U., Ingham, P. W., McMahon, A. P. and Haffter, P. (1997). Wnt5 is required for tail formation in the zebrafish embryo. *Cold Spring Harb. Symp. Quant. Biol.* **62**, 227-234.

Rocheleau, C. E., Downs, W. D., Lin, R., Wittmann, C., Bei, Y., Cha, Y. H., Ali, M., Priess, J. R. and Mello, C. C. (1997). Wnt signaling and an APC-related gene specify endoderm in early C. elegans embryos. *Cell* **90**, 707-716.

Rocheleau, C. E., Yasuda, J., Shin, T. H., Lin, R., Sawa, H., Okano, H., Priess, J. R., Davis, R. J. and Mello, C. C. (1999). WRM-1 activates the LIT-1 protein kinase to transduce anterior/posterior polarity signals in C. elegans. *Cell* **97**, 717-726.

Sepich, D. S., Myers, D. C., Short, R., Topczewski, J., Marlow, F. and Solnica-Krezel, L. (2000). Role of the zebrafish trilobite locus in gastrulation movements of convergence and extension. *Genesis* **27**, 159-173.

Shin, T. H., Yasuda, J., Rocheleau, C. E., Lin, R., Soto, M., Bei, Y., Davis, R. J. and Mello, C. C. (1999). MOM-4, a MAP kinase kinase kinase-related protein, activates WRM-1/LIT-1 kinase to transduce anterior/posterior polarity signals in C. elegans. *Mol. Cell* **4**, 275-280.

Tada, M., Concha, M. L. and Heisenberg, C. P. (2002). Non-canonical Wnt signalling and regulation of gastrulation movements. *Semin. Cell Dev. Biol.* **13**, 251-260.

Taylor, J. S., Van de Peer, Y., Braasch, I. and Meyer, A. (2001). Comparative genomics provides evidence for an ancient genome duplication event in fish. *Philos. Trans. R. Soc. Lond. B Biol. Sci.* **356**, 1661-1679.

Thorpe, C. J., Schlesinger, A., Carter, J. C. and Bowerman, B. (1997). Wnt signaling polarizes an early C. elegans blastomere to distinguish endoderm from mesoderm. *Cell* **90**, 695-705.

Thorpe, C. J., Schlesinger, A. and Bowerman, B. (2000). Wnt signalling in Caenorhabditis elegans: regulating repressors and polarizing the cytoskeleton. *Trends Cell Biol.* **10**, 10-17.

Topczewski, J., Sepich, D. S., Myers, D. C., Walker, C., Amores, A., Lele, Z., Hammerschmidt, M., Postlethwait, J. and Solnica-Krezel, L. (2001). The zebrafish glypican knypek controls cell polarity during gastrulation movements of convergent extension. *Dev. Cell* **1**, 251-264.

Turner, D. L. and Weintraub, H. (1994). Expression of achaete-scute homolog 3 in Xenopus embryos converts ectodermal cells to a neural fate. *Genes Dev.* **8**, 1434-1447.

Ulrich, F., Concha, M. L., Heid, P. J., Voss, E., Witzel, S., Roehl, H., Tada, M., Wilson, S. W., Adams, R. J., Soll, D. R. et al. (2003). Slb/Wnt11 controls hypoblast cell migration and morphogenesis at the onset of zebrafish gastrulation. *Development* **130**, 5375-5384.

van de Water, S., van de Wetering, M., Joore, J., Esseling, J., Bink, R., Clevers, H. and Zivkovic, D. (2001). Ectopic Wnt signal determines the eyeless phenotype of zebrafish masterblind mutant. *Development* **128**, 3877-3888.

Veeman, M. T., Axelrod, J. D. and Moon, R. T. (2003). A second canon. Functions and mechanisms of beta-catenin-independent Wnt signaling. *Dev. Cell* **5**, 367-377.

Verheyen, E. M., Mirkovic, I., MacLean, S. J., Langmann, C., Andrews, B. C. and MacKinnon, C. (2001). The tissue polarity gene nemo carries out multiple roles in patterning during Drosophila development. *Mech. Dev.* **101**, 119-132.

Yamashita, S., Miyagi, C., Carmany-Rampey, A., Shimizu, T., Fujii, R., Schier, A. F. and Hirano, T. (2002). Stat3 controls cell movements during zebrafish gastrulation. *Dev. Cell* **2**, 363-375.